

Mössbauer Spectra of Mixed Crystals; Diamagnetically Substituted Yttrium Iron Garnet in the Critical Region

J. M. D. Coey*

Department of Physics, University of Manitoba, Winnipeg 19, Canada

(Received 3 April 1972)

There is a range of temperature where the Mössbauer spectra of $^{57}\text{Fe}^{3+}$ in diamagnetically substituted magnetically ordered iron oxides show broad lines and may be reproduced by local-molecular-field theory. The lines can exhibit a well-defined structure if the number of neighboring cation sites is less than six, and the spectra can then be used to determine whether the cation distribution is random. Such is the case for $\text{Y}_3(\text{Fe}_{1-x}\text{Sc}_x)_2[\text{Fe}]_3\text{O}_{12}$ with $x=0.10$ and 0.25 . The site preferences of other trivalent cations in yttrium iron garnet (YIG) are measured, including Rh^{3+} which goes onto a sites. At higher temperatures, central peaks appear in the spectra of mixed oxides, and they grow at the expense of the magnetically split spectrum until it finally disappears at T_c . The spectra of $\text{Y}_3(\text{Fe}_{0.75}\text{Sc}_{0.25})_2[\text{Fe}]_3\text{O}_{12}$ were studied in and around this broad critical region. An applied field produces increased hyperfine splitting, which is correlated with the static magnetic susceptibility. The mixed spectra cannot be explained by a range of ordering temperatures in different parts of the crystal, or by independent relaxation of the ionic spins. Short-range collective behavior is indicated, with coupled moments of $(10^2-10^4)\mu_B$ around T_c . A computer study of the geometry of the random lattice shows that there is no tendency to form localized clusters of the right size. The short-range order is probably evanescent.

I. INTRODUCTION

The Mössbauer effect of ^{57}Fe in mixed oxides has been observed by many workers in the last few years. The systems studied, in which some of the magnetic cations are replaced by nonmagnetic ones, include $\alpha\text{Fe}_2\text{O}_3$ with rhodium,^{1,2} gallium,³ or titanium⁴ substitutions; Fe_3O_4 with calcium,⁵ zinc,⁶ gallium,⁷ or vacancies⁸; ferrites such as CoFe_2O_4 ,^{9,10} MnFe_2O_4 ,¹¹ and NiFe_2O_4 ¹²⁻¹⁴ with zinc and several others¹⁵⁻²¹; and also a variety of garnets.²²⁻²⁶

Some general features emerge from this mass of data. The Mössbauer spectrum of ferric ions in a diamagnetically substituted iron oxide belongs to one or another of the following four categories, depending on the temperature T and the nonmagnetic concentration x .

- (i) $T \approx 0$. The spectrum is magnetically split and resembles that of the pure oxide ($x=0$) except that the lines, though sharp, are broadened by up to 0.5 mm/sec.
- (ii) $T_b > T > 0$. The hyperfine splitting decreases as T increases, and the outer lines in particular become broad and asymmetric and may show structure.
- (iii) $T_c > T > T_b$. Central peaks begin to appear at T_b having the form of the paramagnetic spectrum [region (iv)]. As $T \rightarrow T_c$ they increase in intensity at the expense of the magnetically split spectrum, which frequently becomes ill defined.
- (iv) $T > T_c$. All trace of magnetic hyperfine splitting disappears. This behavior is illustrated in Figs. 7 and 8 for $T > 0$.

Much of this paper will be concerned with the critical region iii where mixed spectra occur. The range of temperature ($T_c - T_b$) decreases with decreasing x , but it has been found to be nonzero even in some pure compounds.²⁷⁻³¹ In many mixed systems, T_c decreases linearly with the diamagnetic concentration. The variation of T_b/T_c in such a case² is shown in Fig. 1 for $(\text{Fe}_{1-x}\text{Rh}_x)_2\text{O}_3$, where the four distinct regions of temperature are indicated.

In ionic compounds the magnetic interactions are predominantly short range, and one must therefore seek explanations for the differences between the Mössbauer spectra of pure and substituted oxides in the nearest-neighbor cation environments of the iron ions. Pure compounds with no chemical disorder have only as many distinguishable environments as there are inequivalent lattice sites, taking crystallographic and magnetic symmetry into consideration, and there is generally a distinct spectrum from each site. In mixed crystals, however, there are many different nearest-neighbor environments possible for the iron ions in a given site, all with different numbers and arrangements of magnetic and nonmagnetic neighbors. The simplest situation occurs when the n nearest-neighbor cation sites are equivalent, and belong to the same magnetic sublattice. Then the probability of finding an iron ion with z magnetic and $(n-z)$ nonmagnetic neighbors is

$$P_n(z) = \frac{n!}{z!(n-z)!} (1-x)^z x^{(n-z)}. \quad (1)$$

Some workers^{7,11} have attempted to verify Eq.

(1) by analyzing their spectra from region ii as the superposition of several hyperfine patterns, each one corresponding to a different value of z , but this procedure is uncertain in the spinels studied because the subspectra for different z are not resolved. Nevertheless, we shall show theoretically and experimentally in Secs. II and III that it is possible to resolve the subspectra in certain circumstances, and that the Mössbauer effect can then be used to measure the randomness of the cation distribution. An alternative approach² is to assume a random distribution, and to use Eq. (1) as the basis of the data analysis. This procedure is only justified if the solid solution is between two oxides with identical structures and similar lattice parameters, containing cations of the same valence and ionic radius with weak direct interactions.

The effects observed in the four regions defined above are due to different dominant physical processes.

At absolute zero the iron nuclei in the various environments will experience different hyperfine fields because the cation-cation bonding, dipolar field, zero-point spin deviation³² and supertransferred hyperfine interaction³³ all depend on the numbers of each type of cation neighbor. These effects are all small, but the latter usually predominates. This region will not be discussed further here.

The temperature dependence of the spectrum up to T_p is a reflection of the different temperature dependence of the magnetization of iron ions in different magnetic environments. We have found that these spectra can be reproduced by a simple local-molecular-field theory,³⁴ and that the shape of the spectrum will give information about the strength of the exchange interactions.^{2,19} An improved version of the theory is noted in Sec. II, and a study of the geometry of the random lattice is described which sets the limits to its validity.

Several explanations for the central peaks in the critical region have been advanced. They may show that magnetically ordered and disordered regions coexist in the same crystal, a range of ordering temperatures due to local inhomogeneity.³⁵ Alternatively, they could be caused by a relaxation of the iron spins in a time comparable to the Larmor precession time, $\tau_L \approx 10^{-8}$ sec, whether by individual spin flips,^{30,36} or collective "superparamagnetic" flipping.²⁹ An attempt is made in Sec. IV to distinguish between these hypotheses by analyzing the effect of an applied magnetic field on the Mössbauer spectra of substituted garnets in the critical region, and the measurements are extended above T_c , into region iv. Some data are also presented which suggest that sample preparation technique influences the range $T_c - T_p$ in pure YFeO_3 .

The experimental results and the definition of the ordering temperature in a mixed crystal are discussed in Sec. V, and the main conclusions are then set out in Sec. VI.

II. RANDOM LATTICE

A. Geometry

The magnetic properties of mixed crystals depend on the geometry of the cation distribution. In order to understand the main features of the geometry of a random array of magnetic and nonmagnetic ions, we set up two arrays in the computer. One was a $20 \times 20 \times 20$ simple-cubic lattice with $n=6$, and the other a 90×90 square lattice with $n=4$. Each was populated at random, with $(1-x)$ as the probability for occupation of any particular site. The sizes of the clusters linked by nearest-neighbor paths were then determined, imposing periodic boundary conditions. Tables I and II show the percentages of the occupied sites (magnetic ions) which are members of clusters of various sizes for a complete range of x , the over-all concentration of vacant sites (nonmagnetic ions).

In these lattices, if a cluster contains more than 500 points, it is assumed that in an infinite lattice it would be infinite in extent, although all the occupied sites will only belong to it when $x=0$. The results shown in Tables I and II may be summarized in the following way. When $x \lesssim (n-2)/n$, almost all the occupied sites belong to the bulk cluster, and the remaining few are isolated, or else belong to very small clusters. There is *no tendency to form clusters of intermediate size* because such a cluster would have a large number of adjacent sites, and the probability for at least one of them to be occupied is overwhelming. When

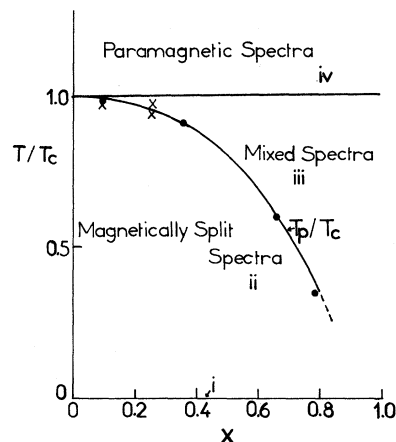


FIG. 1. Regions where four different types of Mössbauer spectra of diamagnetically substituted iron oxides are observed. Dots, $(\text{Fe}_{1-x}\text{Rh}_x)_2\text{O}_3$ (Ref. 2); crosses, this work.

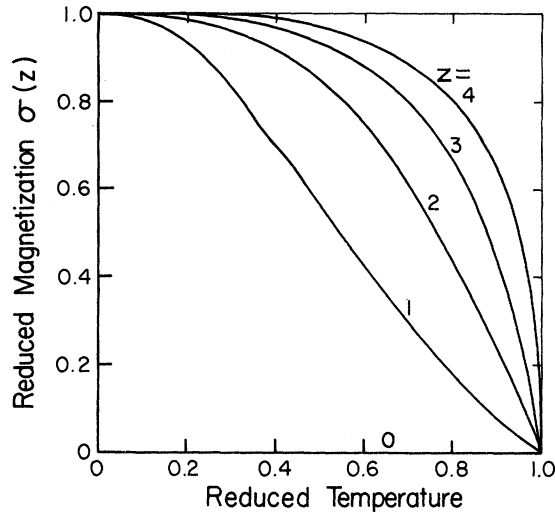


FIG. 2. Magnetization of ions in different environments in a mixed crystal with 0, 1, . . . , 4 magnetic neighbors, calculated from local-molecular-field theory with $x=0.5$ and $n=4$.

an average over all the iron sites in the bulk cluster. The magnetization of the central ion with z neighbors is given by the Brillouin function

$$\bar{S}_z(z) = S \mathfrak{B}_s [g \mu_B S H(z) / kT] . \quad (3)$$

Consistent solutions of (2) and (3) for the reduced magnetization curves of iron in different nearest-neighbor environments may be found: $\sigma(z, T) = \bar{S}_z(z, T) / S$. The corresponding Mössbauer spectra have been calculated,³⁴ assuming the hyperfine field $H_{hf}(z) \propto \bar{S}_z(z)$.³⁹ It is necessary to allow each molecular field $H(z)$ to take a small range of values, because the nearest neighbors of the central ion can themselves have a range of nearest-neighbor environments. Hence the lines in each hyperfine pattern corresponding to a different value of z are broadened.

In the above treatment, the bulk cluster is divided into a central ion, whose interactions are considered explicitly, and the rest of the ions, which are treated in an average way. The average magnetization of all the central ions must be the same as that of the ions in the rest of the bulk cluster. An improvement is to treat the central ion, its shell of interacting neighbors, and the rest of the crystal differently. The ions in the shell have one neighbor whose magnetization is known exactly, namely the central ion, and their remaining interactions have to be treated in an average way. Instead of (2) and (3) we find⁴⁰

$$\sigma(z) = \mathfrak{B}_s \left[\frac{2zJS^2}{kT} \mathfrak{B}_s \left(\frac{2JS^2}{kT} [(\langle z \rangle - 1) \langle \sigma \rangle + \sigma(z)] \right) \right] . \quad (4)$$

The main difference between the two treatments is that (4) gives more widely separated magnetiza-

tion curves close to T_c . The predictions differ little when $T/T_c \lesssim 0.5$. A typical calculation from (4) for the case $n=4$, $x=0.5$ is shown in Fig. 2.

Whether or not the separate hyperfine patterns for different environments are well resolved depends on n and T . Adjacent $\sigma(z)$ curves will be more widely separated the smaller n and the higher T . However, the line broadening due to the distribution of environments for the z neighbors is smallest when the number of occupied cation sites surrounding the neighbors is large, or constant. The best conditions for observing resolved subspectra are found in a two-sublattice structure with iron on one sublattice, and a random distribution of magnetic and nonmagnetic ions on the other. The coordination number of the iron sublattice should be less than 6, for all the systems studied so far have $n \geq 6$ (or else the neighbors do not all have the same spin direction²¹) and in none of them have well-resolved hyperfine patterns been seen for different values of z . Conditions are more favorable in the garnets with a -site substitutions, where $n=4$.

In a two-sublattice structure, Eqs. (2)–(4) must be modified, and terms may be added to represent intrasublattice interactions in the two molecular fields. The predictions are similar to those of the simple model provided the intersublattice exchange is dominant. Further discussion is given in Sec. V.

The molecular field theory predicts a unique ordering temperature for the whole lattice, because the molecular field is formally equivalent to an infinite-range interaction.⁴¹ Furthermore, T_c decreases linearly with x if the average $\langle \dots \rangle$ is taken over all the ions in the lattice. Calculations by cluster methods⁴² closely resemble the molecular-field-theory results.

With strictly nearest-neighbor interactions the theory should only be applied to the bulk cluster, when it exists. Then

$$T_c(x) = T_c(0)(1-x)/f_\infty , \quad (5)$$

where f_∞ is the fraction of the iron ions belonging to the bulk cluster.

The theory is able to reproduce the spectra throughout most of region ii,^{2,34} and may even be applied when $x > x_c$ provided the magnetic interactions extend beyond nearest neighbors. It fails, however, in region iii because the molecular field is never sufficiently small to give sharp central peaks, except in $z=0$ environments. They must be due either to macroscopic inhomogeneity or dynamic effects.

III. MÖSSBAUER SPECTRA AND CATION DISTRIBUTION IN DIAMAGNETICALLY SUBSTITUTED YIG

$Y_3Fe_5O_{12}$ is a ferrimagnetic oxide with three cation sites. The formula may be written

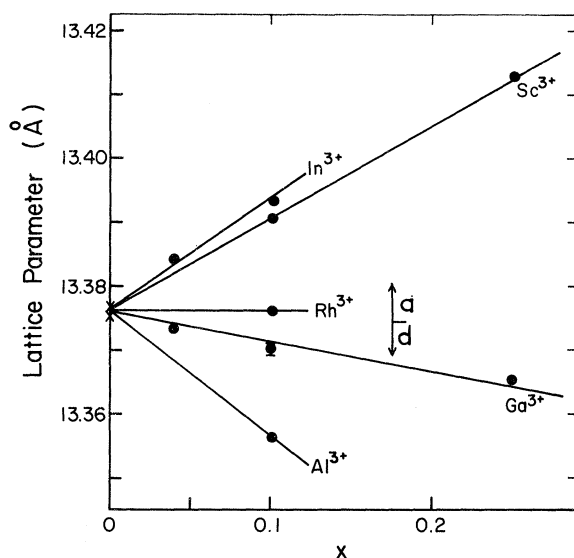
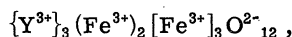
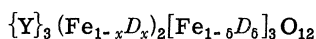


FIG. 3. Lattice parameters of diamagnetically substituted yttrium iron garnet.

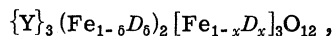


where the different brackets refer to dodecahedral (*c*), octahedral (*a*), and tetrahedral (*d*) interstices in the oxygen lattice. Yttrium is diamagnetic, and strong *a-d* superexchange couples the two iron sublattices antiparallel, giving a ferrimagnetic spin arrangement with a moment of about $5\mu_B$ per formula at low temperatures. Each *a* site has 6 neighbors on the *d* sites, whereas each *d* site has 4 on the *a* sites.

Several trivalent substitutions for iron are known,⁴³ and the site preferences of various ions in YIG have been established.⁴⁴ We will write the formulas of the diamagnetically substituted garnets, $Y_3Fe_{5-t}D_tO_{12}$, as



or



depending on whether D^{3+} has an *a*- or *d*-site preference.

Two things must be specified besides *t*, to define the cation distribution. They are (a) the fraction *f* of the diamagnetic ions on their preferred site; $f = cx/t$, where $t = cx + (5 - c)\delta$ and $c = 2$ or 3 , and (b) the randomness of the distribution of Fe and *D* in a given sublattice.

A. Sample Preparation; Mössbauer Spectra

Samples of YIG were prepared containing small amounts of diamagnetic substitution. Y_2O_3 , Fe_2O_3 , and D_2O_3 were dried and mixed in the required proportions, with $D = Al, Ga, In, Rh, \text{ or } Sc$. The

Y_2O_3 and Fe_2O_3 were spectroscopic grade, and the purity of the other oxides was better than 99.99% except for Rh_2O_3 ,⁴⁵ which was 99.5% pure. One gram of each mixture was pelleted and pre-fired for 12 h at 950 °C in air. The samples were reground, fired finally for 10 h at 1450 °C in oxygen, and then cooled rapidly to room temperature. The sample containing Rh_2O_3 , however, was fired at 1400 °C for only 2 h, but weak rhodium lines were found in the powder pattern. All the other samples showed only x-ray lines belonging to the garnet structure, and the lattice parameters, plotted in Fig. 3, are in agreement with values in the literature.⁴³ The horizontal axis assumes that cations which dilate the lattice are in octahedral sites, and those which contract it are in tetrahedral sites. This assumption is examined below.

The room-temperature Mössbauer spectra of YIG, pure and with 10 site-% substitution, are shown in Fig. 4. The spectrum of pure $Y_3Fe_5O_{12}$ is the superposition of six-line patterns from *a* and *d* sites with an area ratio 2:3. The *a*-site pattern having the larger hyperfine field shows substructure on account of the quadrupole interaction.⁴⁶ The garnets with Ga and Al substitution show broad *a*-site lines, whereas those with Sc, In, and Rh have outer *d*-site lines which are distinct doublets.

It was impossible to predict the site preference of Rh^{3+} from steric considerations, because it does not significantly change the lattice parameter, yet it is clear from Fig. 4(f) that some Rh^{3+} has entered the lattice on the *a* sites. This is consistent with the strong preference of Rh^{3+} for an octahedral site, and low-spin state, found in spinels.⁴⁷

B. Cation Distribution

The fraction *f* can be deduced from the area ratio of the Mössbauer patterns of iron in *a* and *d* sites, provided they are sufficiently well resolved. Either the spectra from region iv (above T_c) may be used²⁶ or else magnetically split spectra from regions i and ii, where the line broadening and overlap is unimportant. The magnetically split spectra of Ga- and In-substituted garnets resemble the one in Fig. 4(a) at 4.2 °K, but the spectra of pure and Sc-substituted YIG become very complex below about 60 °K, and the *a*- and *d*-site patterns overlap, perhaps as a result of a change of magnetic axis away from [111],⁴⁸ or else a distortion of the lattice.

When deriving *f* from the spectra, two corrections may have to be made. First, the recoilless fractions for ^{57}Fe on *a* and *d* sites do not have exactly the same temperature dependence,⁴⁹ and second, absorption corrections must be made when the absorber is not thin.⁵⁰ The corrected values of *f* are given for two of the samples in Table III. Al and Ga prefer *d* sites, whereas In and Sc prefer *a*

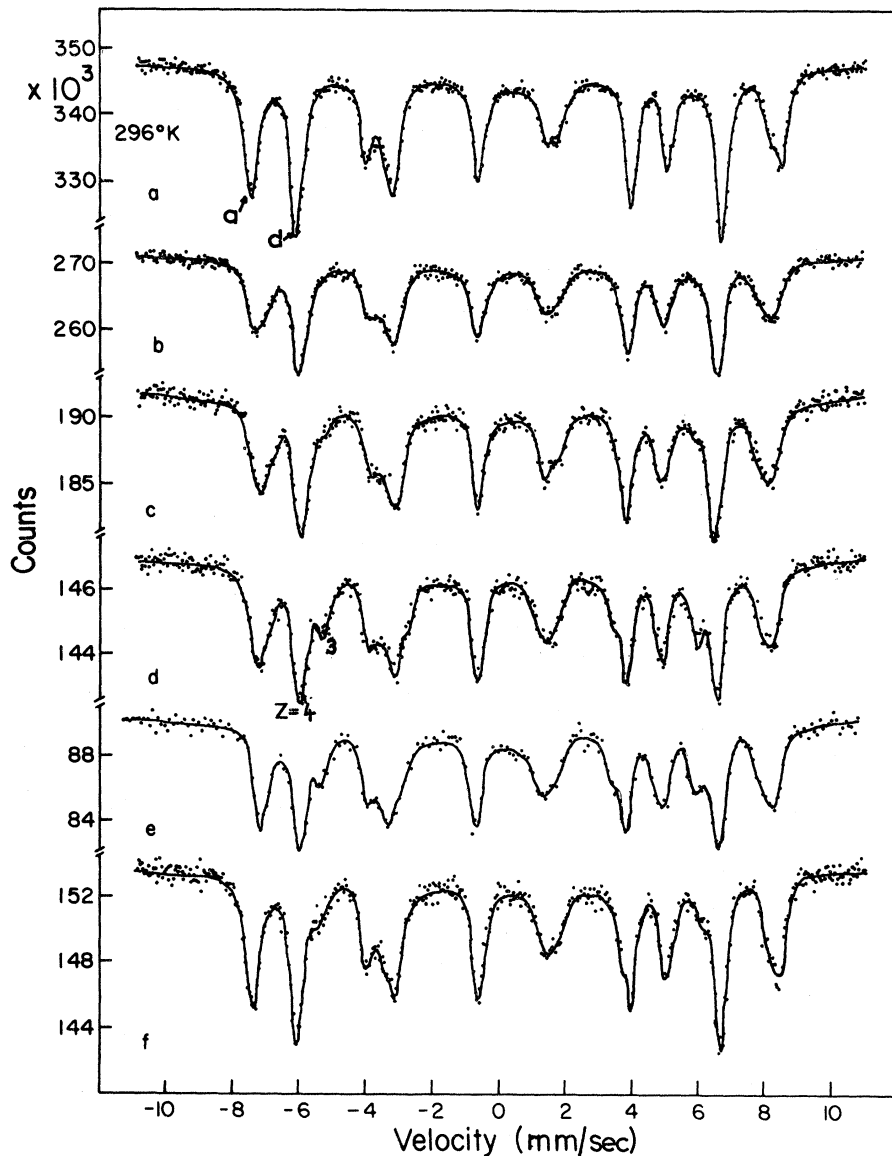


FIG. 4. Mössbauer spectra at 296 °K of (a) $Y_3Fe_5O_{12}$, (b) $Y_3Fe_{4.7}Ga_{0.3}O_{12}$, (c) $Y_3Fe_{4.7}Al_{0.3}O_{12}$, (d) $Y_3Fe_{4.8}Sc_{0.2}O_{12}$, (e) $Y_3Fe_{4.8}In_{0.2}O_{12}$, (f) $Y_3Fe_{5-t}Rh_tO_{12}$.

sites, the preferences of Sc and Ga being particularly strong.

It is possible to define the cation distribution completely, by saying whether it is random or not, in the Sc- and In-substituted garnets. The two d -site patterns in Figs. 4(d)–4(f) are identified with $Fe^{3+}(d)$ having 4 and 3 $Fe^{3+}(a)$ neighbors. If the distribution was random, the intensity ratio would be 1 : 0.44, according to Eq. (1) with $x = 0.10$. The observed ratios are 1 : 0.44, 1 : 0.38, and 1 : 0.22 (± 0.05) for the spectra of Figs. 4(d)–4(f). No conclusion can be drawn from the third ratio, because not all of the rhodium has entered the garnet lattice, but the other two show that the Sc distribution is random, and that In has a slight tendency to form clusters.

The spectrum of the Al-substituted garnet [Fig.

4(c)] has a slight shoulder on the inner edges of lines 1 and 6 of the d -site pattern, but this is not evident for Ga. We deduce that about 20% of the Al, but no more than 5% of the Ga, is on a sites. This is consistent with the data in Table III, and agrees with Czerlinsky's²⁶ results, unexpected from steric considerations, that Al has a weaker d -site preference than Ga in YIG.

The distribution of Sc ions was tested for ran-

TABLE III. Fraction of diamagnetic ions on their preferred sites.

	f	
$Y_3Fe_{4.5}Sc_{0.5}O_{12}$	0.97 ± 0.05	(a)
$Y_3Ga_{4.25}Ga_{0.75}O_{12}$	0.91 ± 0.05	(d)

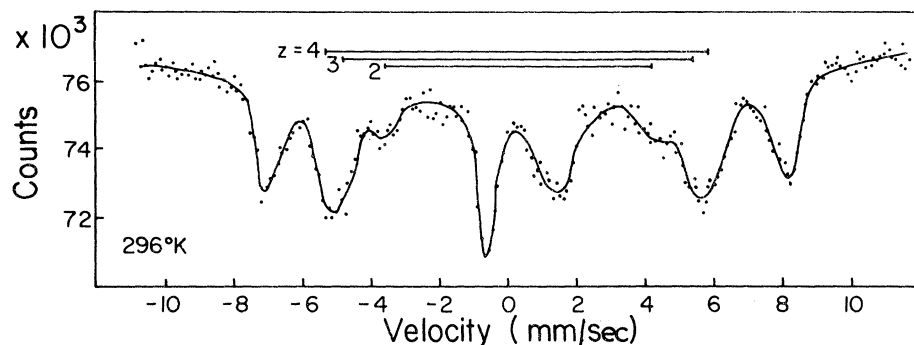


FIG. 5. Mössbauer spectrum of $Y_3(Fe_{0.75}Sc_{0.25})_2[Fe]_3O_{12}$ at 296 °K in an applied field of 20 kOe. The bars show the positions of the outer lines of the spectra of d -site iron with different numbers of a -site neighbors.

domness at another concentration, $x=0.25$. The room-temperature spectrum (Fig. 7) cannot be used directly because the $Fe^{3+}(d)$, $z=2$ pattern overlaps the inner lines of the $Fe^{3+}(a)$ spectrum. However a 20-kOe field aligns all the spins parallel to the γ direction, and removes lines 2 and 5 from all the patterns, giving the spectrum shown in Fig. 5. The probabilities $P_4(z)$ are 0.32, 0.42, 0.21, and 0.05 for $z=4, 3, 2, 1$. The lines indicated are identified with iron in the $z=2$ environment, and their intensity is $31 \pm 5\%$ of the intensity of the outer lines of the d -site pattern, in agreement with 28% expected from a random distribution. Many of the measurements in the critical region were made on this material.

There is no sign of any canting of the d -site moments with this concentration of scandium,^{43,51} and none is expected from the discussion in Sec. V.

IV. CENTRAL PEAKS IN THE MÖSSBAUER SPECTRA OF MAGNETICALLY ORDERED COMPOUNDS

A. Pure and Diamagnetically Substituted YIG

The temperature dependence of the Mössbauer spectrum of pure $Y_3Fe_5O_{12}$ above room temperature is shown in Fig. 6. The ordering temperature, taken as the temperature at which the magnetic hyperfine splitting goes to zero, is 553 °K. There is no sign of the paramagnetic pattern persisting at 550 °K, so that $T_p/T_c > 0.995$.⁵²

The situation is quite different for YIG with 25 site-% of Sc and Ga. The spectra are shown in Figs. 7 and 8. It is clear that for both compounds there is a significant region where mixed spectra occur. If T_p is taken as the temperature at which the three-line paramagnetic pattern becomes distinctly visible, and T_c as the temperature at which the last trace of magnetic splitting has disappeared, then $T_c = 450$ °K and $T_p/T_c = 0.933$ for $Y_3(Fe_{0.75}Sc_{0.25})_2[Fe]_3O_{12}$ and $T_c = 467$ °K and $T_p/T_c = 0.975$ for $Y_3(Fe)_{2}[Fe_{0.75}Ga_{0.25}]_3O_{12}$. It is interesting that the central peaks appear at a lower absolute and reduced temperature in the Sc garnet than in the Ga one, even though the fraction of non-magnetic ions is greater in the latter, and the site-% substitution is the same in each. It seems that

they are more likely to appear in structures with a lower magnetic coordination, since n is 4 in the first case, and 6 in the second.

B. $YFeO_3$

Central peaks have been reported in the Mössbauer spectra of the rare-earth orthoferrites just below their ordering temperature.^{28,53} In view of the different results obtained by different investigators in FeF_3 ,^{27,54} which may be due to small amounts of impurity, it seemed worthwhile making measurements on highly pure $YFeO_3$. The starting oxides contained less than 10 ppm of impurity. After pre-firing for 4 h at 900 °C, the material was ground, pelleted, and then divided into two. The two halves were fired at 1400 °C for 10 h, one in an atmosphere of oxygen, and the other in nitrogen.

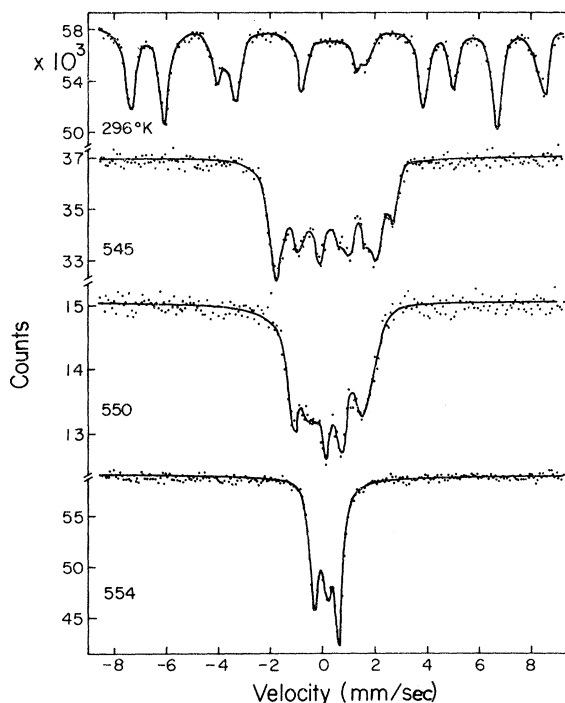


FIG. 6. Mössbauer spectra of $Y_3Fe_5O_{12}$ at different temperatures.

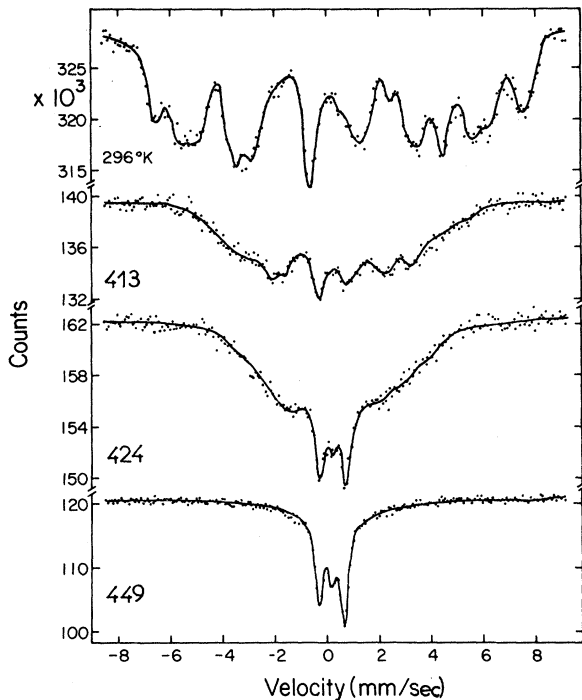


FIG. 7. Mössbauer spectra of $Y_3(Fe_{0.75}Sc_{0.25})_2[Fe]_3O_{12}$ at different temperatures.

The temperature dependence of the hyperfine field was identical in both samples, and the ordering temperature was 647.2 °K for them both. Central peaks are found in both samples, as may be seen in Fig. 9, but there is a slight difference. In the oxygen-fired sample, $T_p/T_c = 0.996$, whereas in the nitrogen-fired sample $T_p/T_c = 0.998$. The two spectra at 645.3 °K may be compared directly. It is not known what effect of firing conditions on the microscopic structure causes the peaks to appear.

C. $Y_3(Fe_{0.75}Sc_{0.25})_2[Fe]_3O_{12}$ in Applied Field

In order to decide whether the central peaks in the Mössbauer spectra below T_c are due to paramagnetic iron, or some form of relaxation process which preserves short-range order, spectra were obtained for one compound in the vicinity of its ordering temperature in an applied field. A specially constructed furnace was used which fits into a 5-cm room-temperature bore of a 50-kOe superconducting magnet.⁵⁵ The temperature stability and uniformity was 0.5 °K.

In Fig. 10, the spectra are shown at temperatures in the range 436–479 °K in the absence and presence of a 10-kOe applied field. The interesting feature of the data is that the 10-kOe field is able to enhance greatly the magnetic splitting of the hyperfine pattern and reduce the fraction of the absorption in the paramagnetic pattern. At 447 °K, three degrees below the temperature

where the hyperfine splitting disappears in zero field, 10 kOe will induce a hyperfine splitting of up to 160 kOe, corresponding to $\langle\sigma\rangle = 0.3$. The spectra at 479 °K are truly paramagnetic in that the applied field simply produces the broadening of the lines which corresponds to 10 kOe. These may be compared with the series of spectra shown in Fig. 11, taken at 457 °K, seven degrees above T_c , in several different applied fields.

It is difficult to analyze the spectra of the mixed crystals near T_c precisely, but the following procedure was adopted. The spectrum was divided into a paramagnetic part which is only slightly field dependent, and a magnetically ordered part, for which an average hyperfine field H_{hf}^{av} could be deduced. The fraction of the absorption in the magnetically split pattern was F . This fraction is 0.60 ± 0.05 for the spectra of Figs. 11(b)–11(d) and 0 for the spectrum of Fig. 11(a). The average polarization $\langle\sigma\rangle$ of an iron ion in the crystal is then taken to be

$$\langle\sigma\rangle = 5FH_{hf}^{av} / [2H_{hf}^a(H_{ap}, 0) + 3H_{hf}^d(H_{ap}, 0)]. \quad (6)$$

The denominator is obtained from the 4.2 °K spectrum. The variation of $\langle\sigma\rangle$ with H_{app} is shown in Fig. 12, together with the variation of the polarization of the magnetically split portion, that is $\langle\sigma\rangle/F$.

In Fig. 13, the variation of $\langle\sigma(T, H_{ap})\rangle$ is given for $H_{ap} = 0$ and $H_{ap} = 10$ kOe. It is remarkable that the ordering temperature, defined by the disappearance of all hyperfine splitting, is about 25 °K higher in a 10-kOe field.

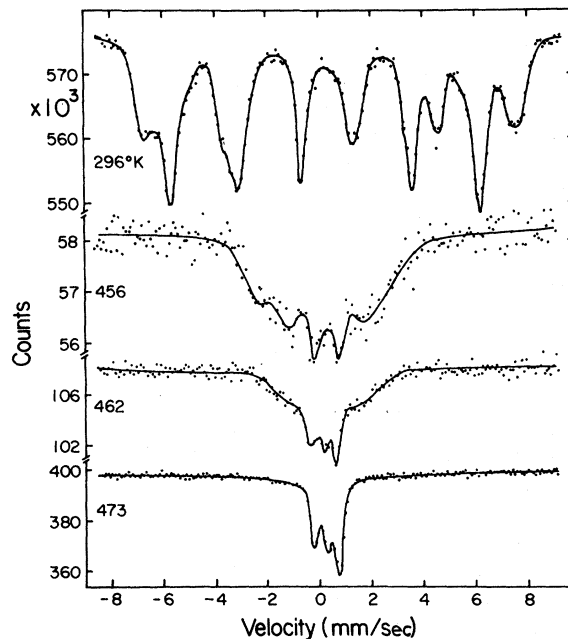


FIG. 8. Mössbauer spectra of $Y_3(Fe)_2[Fe_{0.75}Ga_{0.25}]_3O_{12}$ at different temperatures.

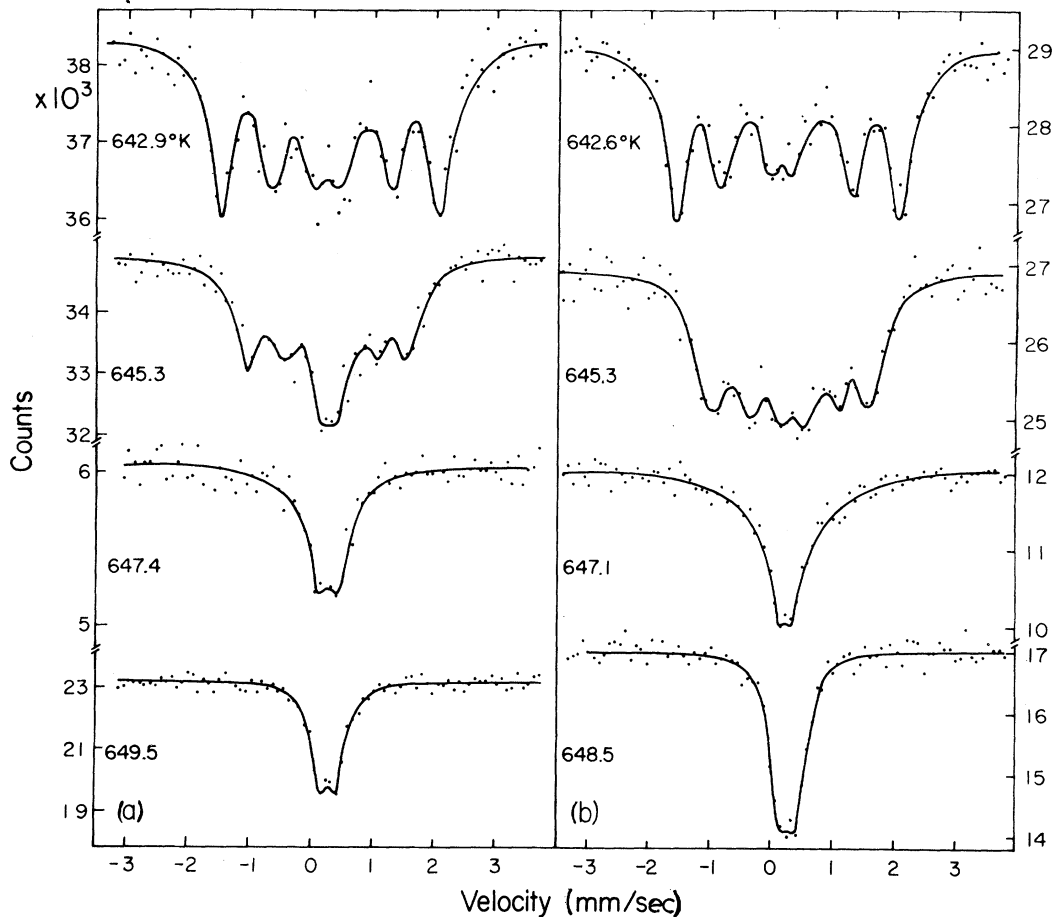


FIG. 9. Mössbauer spectra of YFeO_3 in the vicinity of T_c , (a) fired in an oxygen atmosphere and (b) fired in a nitrogen atmosphere.

Static magnetization measurements were also made on several of the compounds, and magnetic moment at each temperature was found by extrapolating the magnetization in fields of 10–16 kOe to zero field. This method gives an ordering temperature in agreement with that deduced from Mössbauer measurements, only for pure YIG. The values of T_c obtained by the two methods are shown in Table IV, and values of $\langle\sigma\rangle$ deduced from the magnetization in a 10-kOe field are included in Fig. 13.

V. DISCUSSION

We will first consider how far the data of Sec. IV are able to distinguish between the three explanations that have been proposed for the central peaks in region iii, namely, a range of ordering temperature, or individual or collective spin flipping.

In an external applied field H_{ap} the hyperfine field at an $^{57}\text{Fe}^{3+}$ nucleus in a solid with no spontaneous magnetization may be written

$$H_{hf} = H_{ap} - \sigma(H_{ap}, T)H_{hf}(0). \quad (7)$$

$H_{hf}(0)$ is the numerical value of the hyperfine field

at $T=0$ and the minus sign indicates that it is oppositely directed to the ionic spin \bar{S}_z . $\sigma(H_{ap}, T)$ ($=\bar{S}_z/S$) is the ionic polarization averaged over the Larmor precession time. σ is only large for paramagnets near $T=0$, and for magnetically ordered compounds, just above their ordering temperature.

The static ionic polarization, which is proportional to the magnetic susceptibility, will always be less than the σ derived from Mössbauer spectra because of the different characteristic times, but the data in Fig. 13 show that values of $\langle\sigma\rangle$ derived by the two methods agree within 30%.

A virtue of the Mössbauer spectra is that they give an idea of the range of σ for individual ions, and not merely its average value. The near equivalence of magnetic and Mössbauer measurements of $\langle\sigma\rangle$ allows us to examine the hypothesis that the central peaks are due to different parts of the material having different ordering temperatures.

The inverse susceptibility of a two-sublattice ferrimagnet theoretically follows a hyperbola,⁵⁶ and the actual behavior of YIG is similar.⁵⁷ The

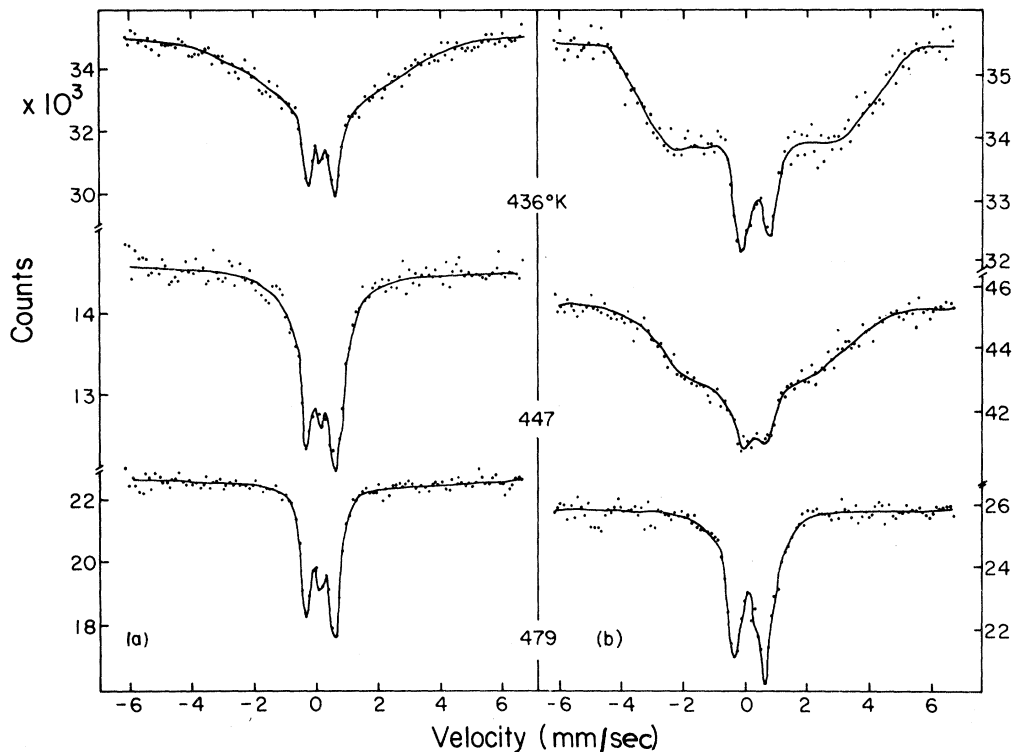


FIG. 10. Mössbauer spectra of $Y_3(Fe_{0.75}Sc_{0.25})_2[Fe]_3O_{12}$; (a) in zero applied field, (b) in an applied field of 10 kOe.

central peaks in $Y_3(Fe_{0.75}Sc_{0.25})_2[Fe]_3O_{12}$ begin to appear at 430 °K. If there is a uniform distribution of ordering temperatures between 430 and 450 °K, and if each region has the same susceptibility above its ordering temperature as $Y_3Fe_5O_{12}$ (but scaled by 1.4, the ratio of the moments at $T = 0^{43}$), then the reduced magnetization induced by a 10-kOe field 7 °K above T_c would be only 0.022. $\langle \sigma \rangle$ derived from the Mössbauer spectrum at 457 °K is 0.13, and from magnetization measurements it is 0.10. Therefore the critical behavior of these mixed oxides cannot be properly explained in terms of a range of ordering temperature. In fact the susceptibility of $Y_3(Fe_{0.75}Sc_{0.25})_2[Fe]_3O_{12}$ around T_c is even greater than it is in pure YIG, and not much less, as a range or ordering temperature would require. The critical isotherm in pure $Y_3Fe_5O_{12}$ has the equation⁵⁸ $M_{T=T_c}(H_{ap}) = 3.75H_{ap}^{1/4,42}$. Fitting a curve with the same exponent through the data of Fig. 12 at 1.016 T_c gives a coefficient of 4.4.

It is possible that the spectra near T_c could arise from ions with a relaxation time for spin flipping of order τ_L .³⁶ If this relaxation was uncorrelated and the ions independent, then the spectra in an applied field would have to be explained by a reduction of the relaxation time by about an order of magnitude. There would then be no reason for the agreement between Mössbauer and magnetization

measurements of $\langle \sigma \rangle$ in 10 kOe. Moreover, the measurements just above T_c indicate that the spins are not uncorrelated, and purely paramagnetic, but that there exists a large degree of short-range order. A high static susceptibility throughout a broad critical region was studied in (NiZn) ferrites by Ishikawa,⁵⁹ and explained in terms of critical superparamagnetism or short-range order. The central peaks found in the Mössbauer spectra of pure²⁹ and mixed crystals¹⁴ have been explained in the same way.

Superparamagnetic particles behave much like single magnetic ions with a very large spin. In a parallel experiment⁶⁰ we determined the effect of an applied magnetic field on the spectra of ultra-fine particles of γFe_2O_3 . At room temperature these particles are superparamagnetic, and the Mössbauer spectrum is a broad single line, indi-

TABLE IV. Ordering temperatures.

	$Y_3Fe_5O_{12}$	$Y_3(Fe_{0.75}Sc_{0.25})_2[Fe]_3O_{12}$
Temperature at which the last trace of magnetic splitting disappears from the Mössbauer spectrum (T_c)	553 °K	450
Temperature at which the static magnetization, extrapolated to $H = 0$, disappears	555	459

cating that the relaxation time τ is close to τ_L . When a large field is applied, a well-developed magnetic hyperfine pattern appears, which can essentially be explained if the magnetization of each particle is given by a Langevin function. The relaxation time need not be changed by the field⁶¹ for hyperfine splitting to be seen. All that is necessary is that the particles should be polarized, and spend more time with their moments parallel to the field than antiparallel, since the splitting depends on \bar{S}_z .

In terms of critical superparamagnetism the spectra of the previous section are explained as follows. Between T_p and T_c the crystal has broken up into magnetically independent regions. The larger ones are stable, but the smaller ones are above their blocking temperature and the net moments fluctuate rapidly compared to τ_L , although there is still a semblance of magnetic order within the regions, which finally disappears well above T_c . As T increases from T_p , the average size of the regions decreases, and so does the fraction of

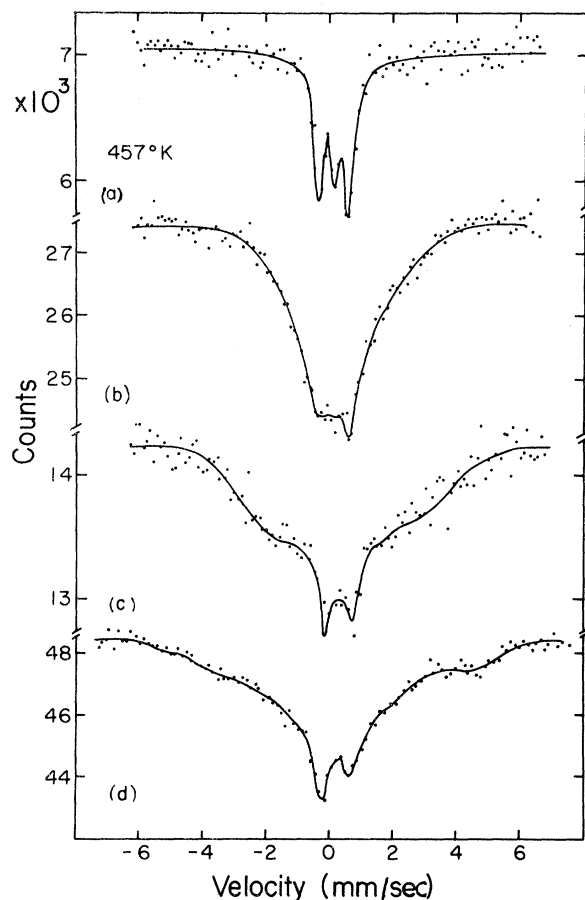


FIG. 11. Mössbauer spectra of $Y_3(Fe_{0.75}Sc_{0.25})_2[Fe]_3O_{12}$ at 457 K in an applied field of (a) 0 kOe, (b) 10 kOe, (c) 30 kOe, and (d) 50 kOe.

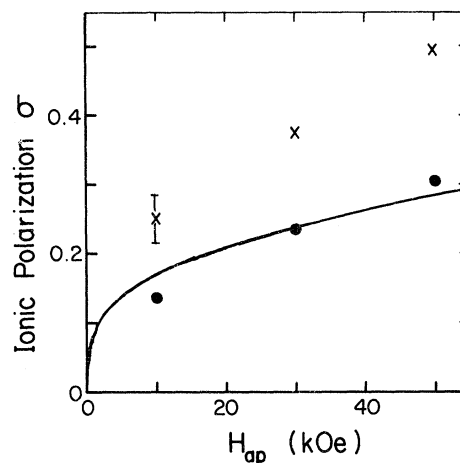


FIG. 12. Average polarization of the iron ions, derived from the spectra of Fig. 11 using dots, the whole spectrum; and crosses, the magnetically split part only.

iron ions in regions with less than the critical volume which gives rise to the central peaks. An estimate of the size of the larger regions just above T_c can be made by fitting a Langevin function through the upper 10-kOe point in Fig. 12. The net spin of the cluster is $1.5 \times 10^4 \mu_B$, and it contains at least 10^5 iron ions, with dimension greater than 100 Å. The smallest cluster have moments of $10^2 \mu_B$, or less. All the data in Fig. 12 cannot be fitted to a single Langevin function because there is such a range of cluster sizes present.

The main difficulty with the model of critical superparamagnetism is that there are no obvious boundaries for the superparamagnetic clusters. The considerations of Sec. II give no indication that the crystal divides itself into clusters of 10^3 – 10^5

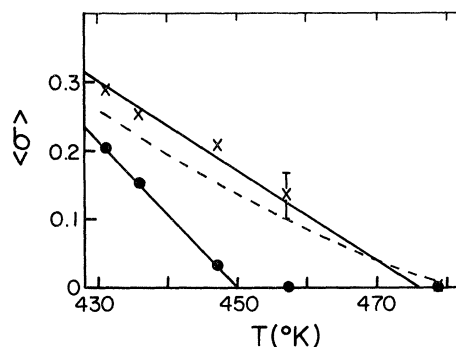


FIG. 13. Average polarization of iron ions in $Y_3(Fe_{0.75}Sc_{0.25})_2[Fe]_3O_{12}$ deduced from Mössbauer spectra; dots taken in zero applied field, crosses taken in an applied field of 10 kOe. Linear extrapolation to $\langle \sigma \rangle = 0$ defines T_c . The broken line is the average polarization of the iron ions deduced from static magnetization measurements in a 10-kOe field.

ions, and with $x=0.25$ the overwhelming majority of the ions belong to the bulk cluster. It is possible that this bulk cluster contains weak points, where it is connected by only a few nearest-neighbor bonds, but these become increasingly improbable as $x \rightarrow 0$. However, there is nothing in the Mössbauer data which requires the superparamagnetic clusters to be localized regions of the crystal. The short-range spin correlation may be evanescent, yet persist for a time longer than τ_L while the direction of the net moment changes many times.

Any definition of T_c will contain a distance and a time over which spin correlations are to be measured. In practice, the time is a property of the measuring technique, and in Mössbauer experiments it is τ_L . The definition of T_c as the temperature at which the last trace of magnetic splitting disappears requires that the relaxation time of an ionic spin is very small, $< 10^{-9}$ sec, but does not exclude instantaneous long- or short-range magnetic order. The range of the order can only be determined from experiments in an applied field. T_c similarly defined in an applied field is the temperature at which the relaxation time is very small, and all short-range order has disappeared.

In static magnetization measurements, the characteristic time is much longer; typically 1 sec, and it is expected that lower values of T_c will normally be found in zero field. However the extrapolation to $H=0$ is likely to give nonzero values of the magnetization in the region where critical superparamagnetism occurs and hence high values of T_c . The raising of the ordering temperature by 25 °K in the 10-kOe field is similarly explained, in terms of the polarization of rapidly relaxing superparamagnetic clusters.

Finally, the treatment given in Sec. II B of a central ion surrounded by magnetic and nonmagnetic neighbors is compared with models developed by other authors for the diamagnetically substituted garnets.

Geller found a decrease in the iron moment extrapolated to 0 °K in garnets with a -site substitutions when $x \gtrsim 0.64$. He proposed a random canting in the unsubstituted sublattice due to competing inter- and intrasublattice interactions.^{43,62} (Similar behavior for the surface ions in ultrafine ferromagnetic particles has recently been suggested.⁶⁰) Geller's localized canting model was developed by Rosencwaig,⁵¹ who estimated $J_{aa}/J_{ad} \approx 0.23$ and $J_{aa}/J_{ad} \approx 0.07$. Significant canting occurs only for ions with $z < 2$ in a -substituted garnets and $z < 1$ in d -substituted garnets. A similar model due to Nowik⁶³ is a limiting case of Rosencwaig's general formulation. He supposes that the spins of d -site iron ions with no a -site iron neighbors ($z=0$) in the

a -substituted garnets are reversed, whereas if $z=1$ they are canted. He makes the point that the hyperfine field will *not* be proportional to the sublattice magnetization in these circumstances.

These effects, however, have no influence on our data analysis because they become important only when the diamagnetic substitution is high enough for environments with $z < 2$ to have an appreciable probability, that is $x \gtrsim 0.35$ for $Y_3(\text{Fe}_{1-x}\text{Sc}_x)_2[\text{Fe}]_3\text{O}_{12}$.

The theory in Sec. II B was given for a ferro- or antiferromagnet with only one exchange interaction. It can be extended in a straightforward way to ferrimagnets, and to include other exchange interactions while retaining a collinear structure.³⁴ Provided the intersublattice interaction dominates, it is reasonable to define the environments of an iron ion by the single parameter z . However, when the inter- and intrasublattice interactions become comparable, one must adopt the approach of the above authors.

Assuming that J_{ad} and J_{aa} are the only important interactions, we took the four sublattice magnetizations from the data of Fig. 5, $\sigma_a=0.84$, $\sigma_d(4)=0.80$, $\sigma_d(3)=0.72$, and $\sigma_d(2)=0.54$, to determine their ratio, using modified versions of Eq. (4). The result is $J_{aa}/J_{ad} \sim 0.1$, but we found previously² that to derive precise values of the exchange constants from local-molecular-field theory, data are needed at several temperatures, or for several different values of x .

It may be noted that high-field Mössbauer experiments on garnets with higher diamagnetic concentrations than those studied here would elucidate the nature of the canting if any.⁶⁴

VI. CONCLUSIONS

In favorable structures it is possible to use the Mössbauer effect to measure not only the cation distribution among different sites, but also to see if the arrangement of a magnetic ion and a nonmagnetic substitution in equivalent sites is random. This was found to be the case in $\{Y\}_3(\text{Fe}_{1-x}\text{Sc}_x)_2[\text{Fe}]_3\text{O}_{12}$ with $x=0.10$ and 0.25. Site preferences found for other trivalent substitutions agree with previous work, and the preference of Rh^{3+} for the octahedral d sites was established.

The central peaks appearing in the Mössbauer spectra of the diamagnetically substituted garnets are not true paramagnetic peaks, due to a range of ordering temperature, but arise from iron in clusters of short-range order, the ionic moment being subject to fast relaxation which is at least partially collective. The size of these clusters is estimated as 10^3 – 10^5 ions just below the temperature at which the last trace of magnetic hyperfine splitting disappears, but they persist even above this temperature. A study of the geometry of the ran-

dom lattice with nearest-neighbor interactions showed no tendency for localized regions of this magnitude to form, and it is suggested that they are evanescent.

ACKNOWLEDGMENT

This work was supported by the National Research Council of Canada.

* Present address: Groupe de Transitions de Phases, Laboratoire de Magnétisme, C. N. R. S. Cedex 166, 38, Grenoble-Gare, France.

¹I. Dészi, Gy Erlaki, and L. Keszthelyi, *Phys. Status Solidi* **21**, K121 (1967).

²J. M. D. Coey and G. A. Sawatzky, *J. Phys. C* **4**, 2386 (1971).

³J. M. Trooster and A. Dymanus, *Phys. Status Solidi* **24**, 487 (1967).

⁴G. Shirane, D. E. Cox, W. J. Takei, and S. L. Ruby, *J. Phys. Soc. Japan* **17**, 1598 (1962).

⁵A. Z. Hryniewicz, D. S. Kulgawczuk, E. S. Mazarek, A. J. Putowka, J. A. Sawicki, and M. E. Wyderko, *Phys. Status Solidi* **b43**, 401 (1971).

⁶D. C. Dobson, J. W. Linnett, and M. M. Rahman, *J. Phys. Chem. Solids* **31**, 2727 (1970).

⁷A. Kostikas, A. Simopoulos, and N. H. J. Gangas, *Phys. Status Solidi* **42**, 705 (1970).

⁸J. M. D. Coey, A. H. Morrish, and G. A. Sawatzky, *J. Phys. (Paris)* **32**, C1-271 (1971).

⁹P. K. Iyengar and S. C. Bhargava, *Phys. Status Solidi* **b46**, 117 (1971).

¹⁰G. A. Pettitt and D. W. Forester, *Phys. Rev. B* **4**, 3912 (1971).

¹¹L. Czer, I. Dészi, I. Gladkih, L. Keszthelyi, D. Kulgawczuk, N. A. Eissa, and E. Sterk, *Phys. Status Solidi* **27**, 131 (1968).

¹²H. Abe, M. Matsumura, H. Yasuoka, A. Hirai, T. Hashi, and T. Fukuyama, *J. Phys. Soc. Japan* **18**, 1400 (1963).

¹³J. M. Daniels and A. Rosencwaig, *Can. J. Phys.* **48**, 381 (1970).

¹⁴P. Raj and S. K. Kulshreshtha, *Phys. Status Solidi* **a4**, 501 (1971).

¹⁵A. Z. Hryniewicz, D. S. Kulgawczuk, and K. Tomalo, *Acta Phys. Polon.* **28**, 423 (1965).

¹⁶G. A. Fatseas and R. Krishnan, *J. Appl. Phys.* **39**, 1256 (1968).

¹⁷B. J. Evans, *Mössbauer Effect Methodology* (Plenum, New York, 1968), Vol. 4, p. 139.

¹⁸E. Wieser, V. A. Povitskii, E. F. Makarov, and K. Kleinstück, *Phys. Status Solidi*, **25**, 607 (1968).

¹⁹G. A. Sawatzky, F. Van Der Woude, and A. H. Morrish, *Phys. Rev.* **187**, 747 (1969).

²⁰P. Raj and S. K. Kulshreshtha, *J. Phys. Chem. Solids* **31**, 9 (1970).

²¹C. Do Dinh, R. Chevalier, P. Burlet, and E. F. Bertaut, *J. Phys. (Paris)* **31**, 401 (1970).

²²I. S. Lyubutin, in *Proceedings of the Conference on the Applications of the Mössbauer Effect, Tihany, 1969* (Akademiai Kiado, Budapest, 1971), p. 467.

²³L. Brossard, R. Krishnan, and G. A. Fatseas, in *Ref. 22*, p. 491.

²⁴J. Piekoszewski and J. Suwalski, in *Ref. 22*, p. 499.

²⁵V. A. Bokov, S. I. Jushchuk, and G. V. Popov, *Solid State Commun.* **7**, 373 (1969).

²⁶E. R. Czerlinsky, *Phys. Status Solidi* **34**, 483 (1969); E. R. Czerlinsky and R. A. Mac Millan, *ibid.* **41**, 333 (1970).

²⁷U. Bertelsen, J. M. Knudsen, and M. Krogh, *Phys. Status Solidi* **22**, 59 (1967).

²⁸M. Eibschütz, S. Shtrikman, and D. Treves, *Phys. Rev.* **156**, 567 (1967).

²⁹L. M. Levinson, M. Luban, and S. Shtrikman, *Phys. Rev.* **177**, 864 (1969).

³⁰F. Van Der Woude and A. J. Dekker, *Phys. Status Solidi* **13**, 181 (1966).

³¹C. E. Johnson, *J. Phys. C* **2**, 1996 (1969).

³²H. P. Van Der Braak and W. J. Caspers, *Phys. Status Solidi* **24**, 733 (1967); H. P. Van Der Braak, *Physica* **42**, 137 (1969).

³³F. Van Der Woude and G. A. Sawatzky, *Phys. Rev. B* **4**, 3159 (1971).

³⁴J. M. D. Coey and G. A. Sawatzky, *Phys. Status Solidi* **b44**, 673 (1971).

³⁵Y. Nakamura, M. Shiga, and N. Shikazono, *J. Phys. Soc. Japan* **19**, 1177 (1964).

³⁶F. Van Der Woude and A. J. Dekker, *Phys. Status Solidi* **9**, 775 (1965).

³⁷M. A. Gilleo, *J. Phys. Chem. Solids* **13**, 33 (1960).

³⁸P. G. de Gennes, P. Laforé, and J. M. Millot, *J. Phys. Chem. Solids* **11**, 105 (1959).

³⁹F. Van Der Woude, G. A. Sawatzky, and A. H. Morrish, *Phys. Rev.* **167**, 533 (1968); H. Pinto, G. Shachar, and H. Shaked, *Solid State Commun.* **8**, 597 (1970).

⁴⁰J. M. D. Coey, PhD thesis (University of Manitoba, 1971) (unpublished).

⁴¹H. E. Stanley, *Introduction to Phase Transitions and Critical Phenomena* (Oxford U. P., New York, 1971), p. 91.

⁴²J. F. Devlin and G. A. Sawatzky (unpublished).

⁴³M. A. Gilleo and S. Geller, *Phys. Rev.* **110**, 73 (1958); S. Geller, H. J. Williams, G. P. Espinosa, and R. C. Sherwood, *Bell Sys. Tech. J.* **43**, 565 (1964).

⁴⁴S. Geller, *J. Appl. Phys.* **31**, 305 (1960).

⁴⁵J. M. D. Coey, *Acta Cryst.* **B26**, 1876 (1970).

⁴⁶C. Alff and G. K. Wertheim, *Phys. Rev.* **122**, 1414 (1961).

⁴⁷G. Blasse, *Philips Res. Rept.* **18**, 383 (1963).

⁴⁸Spectra of two different samples of $Y_3Fe_5O_{12}$ suggest an easy axis closer to [110] than [111] at 4.2 °K. This was not observed by the authors of *Ref. 24*, but Sh. Bashkurov, N. G. Ivoilov, and V. A. Chistyakov, *Fiz. Tverd. Tela* **13**, 689 (1971) [*Sov. Phys. Solid State* **13**, 570 (1971)] have proposed that the easy axis changes with temperature in the range 80–540 °K.

⁴⁹G. A. Sawatzky, F. Van Der Woude, and A. H. Morrish, *Phys. Rev.* **183**, 383 (1969).

⁵⁰G. A. Shirley, M. Kaplan, and P. Axel, *Phys. Rev.* **123**, 816 (1961); U. Shimony, *Nucl. Inst. Meth.* **37**, 348 (1965).

⁵¹A. Rosencwaig, *Can. J. Phys.* **48**, 2857 (1970); **48**, 2868 (1970).

⁵²A complete study of the Mössbauer spectrum of pure YIG in the critical region by A. M. Van Der Kraan and J. J. Van Loef, in *Ref. 22*, p. 519, shows that $T_p/T_c > 0.9995$, and that the critical exponent β for both sub-

lattices increases a few degrees below T_c . Critical superparamagnetism cannot therefore be the cause of the $\beta = \frac{1}{2}$ exponent found near T_c in magnetization measurements.

⁵³J. M. D. Coey, G. A. Sawatzky, and A. H. Morrish, *Phys. Rev.* **184**, 334 (1969).

⁵⁴G. K. Wertheim, H. J. Guggenheim, and D. N. E. Buchanan, *Phys. Rev.* **169**, 465 (1968).

⁵⁵J. M. D. Coey, D. C. Price, and A. H. Morrish, *Rev. Sci. Instr.* **43**, 54 (1972).

⁵⁶L. Néel, *Ann. Phys.* **3**, 317 (1948).

⁵⁷R. Aléonard, J. C. Barbier, and R. Pauthenet, *Comp. Rend. Acad. Sci. Paris* **242**, 2531 (1956).

⁵⁸K. Miyatani and K. Yoshikawa, *J. Appl. Phys.* **41**, 1272 (1970).

⁵⁹Y. Ishikawa, *J. Appl. Phys.* **35**, 1054 (1964).

⁶⁰J. M. D. Coey and D. Khalafalla, *Phys. Status Solidi* **a11**, 229 (1972); J. M. D. Coey, *Phys. Rev. Letters* **27**, 1140 (1971).

⁶¹Weak fields may decrease the relaxation time. [A. Aharoni and R. Bijaoui (unpublished).]

⁶²S. Geller, *Phys. Rev.* **181**, 980 (1969).

⁶³I. Nowik, *Phys. Rev.* **171**, 550 (1968); *J. Appl. Phys.* **40**, 5184 (1969).

⁶⁴D. Lebenbaum and I. Nowik, *Phys. Letters* **31A**, 373 (1970).

Decay of Multiple Spin Echoes in Dipolar Solids

C. H. Wang

Department of Chemistry, The University of Utah, Salt Lake City, Utah 84112

and

John D. Ramshaw

Department of Physics, The University of Utah, Salt Lake City, Utah 84112

(Received 27 December 1971)

In this paper we derive a general expression describing the evolution of the transverse nuclear-spin magnetization for the Ostroff-Waugh multiple-spin-echo experiment in dipolar solids. Our approach consists of expressing the formula for the magnetization at even echoes in a form resembling an ordinary time-correlation function, and then evaluating this quantity by means of Zwanzig's projection-operator technique. For long times, we show that under certain conditions the echo envelope decays exponentially, in agreement with experiment. A general expression is obtained for the time constant T^* associated with the decay. This result may be used to generate an expansion of $1/T^*$ in powers of the cycle time t_c , but there are experimental indications that this expansion is not legitimate and that more complicated t_c dependences can arise. In the case when higher-order correlations decay much more rapidly than lower-order ones, our result reduces to $1/T^* = A t_c^4 \tau_c^0(t_c)$, where A is a quantity related to the sixth moment of the magnetization and $\tau_c^0(t_c)$ is a characteristic correlation time associated with decay of the lowest-order correlation function which enters the problem. The t_c dependence of T^* is then determined by the behavior of $\tau_c^0(t_c)$, and is in general more complex than the proportionality between $1/T^*$ and t_c^6 found previously. This previous result emerges in the case when $\tau_c^0(t_c) = t_c$. Available experimental results suggest that $1/T^*$ is in general a nonanalytic function of t_c , as indicated by the observed proportionality between $1/T^*$ and t_c for Teflon and KAsF_6 . Further experimental results are needed to clarify the nature of this nonanalytic behavior.

I. INTRODUCTION

It was reported^{1,2} that a periodic train of 90° rf pulses can greatly prolong the decay of transverse nuclear spin magnetization in dipolar solids. The effect is observed as a train of multiple spin echoes analogous to (but quite different in character from) the familiar "classical" spin echoes first observed by Hahn.³ A detailed analysis of this effect, including the dependence of the decay time T^* for the echo envelope upon the pulse spacing, was given by Waugh and Wang.⁴ The pulse sequence which gives rise to the effect may be represented symbolically as $P_x, \tau, P_y, (2\tau, P_y)_n$, where

P_α ($\alpha = x, y$) denotes a 90° pulse along the α axis of a reference frame rotating at the Larmor frequency ω_0 ($=\gamma H_0$). The first pulse P_x serves merely to establish a suitable initial condition for the remainder of the sequence. This pulse is followed, after a time τ , by a train of n P_y pulses ($n \sim 10^3$) spaced apart by a time 2τ .

The free induction decay following a single P_x pulse in a dipolar solid decays nonexponentially to zero on a time scale T_2 (T_2 is the normal transverse relaxation time). However, the echo train induced by the action of the subsequent P_y pulses persists for times several orders of magnitude longer than T_2 .^{1,2,4} In fact, by reducing the pulse